10454
NACA TN 4120

TECH LIBRARY KAFB, NM
0066872

NATIONAL ADVISORY COMMITTEE FOR AERONAUTICS

TECHNICAL NOTE 4120

THEORETICAL CALCULATIONS OF SUPERSONIC WAVE DRAG AT ZERO LIFT FOR A PARTICULAR STORE ARRANGEMENT

By Kenneth Margolis, Frank S. Malvestuto, Jr.,
and Peter J. Maxie, Jr.

Langley Aeronautical Laboratory
Langley Field, Va.

Washington
January 1958

AFMDC
TECHNICAL
AFL 2811

TECH LIBRARY KAFB, NM
0066872

NATIONAL ADVISORY COMMITTEE FOR AERONAUTICS

TECHNICAL NOTE 4120

THEORETICAL CALCULATIONS OF SUPERSONIC WAVE DRAG AT ZERO LIFT FOR A PARTICULAR STORE ARRANGEMENT

By Kenneth Margolis, Frank S. Malvestuto, Jr.,
and Peter J. Maxie, Jr.

SUMMARY

An analysis, based on the linearized thin-airfoil theory for supersonic speeds, of the wave drag at zero lift has been carried out for a simple two-body arrangement consisting of two wedgelike surfaces, each with a rhombic lateral cross section and emanating from a common apex. Such an arrangement could be used as two stores, either embedded within or mounted below a wing, or as auxiliary bodies wherein the upper halves could be used as stores and the lower halves for bomb or missile purposes. The complete range of supersonic Mach numbers has been considered and it was found that by orienting the axes of the bodies relative to each other a given volume may be redistributed in a manner which enables the wave drag to be reduced within the lower supersonic speed range (where the leading edge is substantially subsonic). At the higher Mach numbers, the wave drag is always increased. If, in addition to a constant volume, a given maximum thickness-chord ratio is imposed, then canting the two surfaces results in higher wave drag at all Mach numbers. For purposes of comparison, analogous drag calculations for the case of two parallel winglike bodies with the same cross-sectional shapes as the canted configuration have been included. Consideration is also given to the favorable (dragwise) interference pressures acting on the blunt bases of both arrangements.

INTRODUCTION

The magnitude of the supersonic wave drag of complete airplane configurations is known to be dependent not only on the direct drag effects generated by each component part of the configuration but also on the indirect or interference effects introduced by each component on all other components. For airplanes that require external fuel tanks, prominent nacelles, or other auxiliary bodies for storage or bomb and missile purposes, the location of such bodies relative to each other and to other airplane components has been shown to be an important consideration from the standpoint of obtaining low drag. In this connection, reference 1

points out that judicious positioning of the components of a multibody arrangement can give rise to beneficial interference effects that are of sufficient magnitude to allow a volume increase of 25 percent and at the same time actually decrease the wave drag at zero lift. Although the possible increases in other forms of drag (e.g., friction drag, base drag, and drag due to lift) might partially cancel or even completely nullify such reduction in zero-lift wave drag, the importance of positioning auxiliary bodies appears clear.

Inasmuch as interest has been evidenced in the lift and side force of conical stores oriented relative to each other, it was believed worthwhile to consider also the drag problem for a similar arrangement. In order to allow a rigorous analytical solution as well as to simplify the calculations, the present paper treats the case of two simple wedge-type stores, canted relative to each other, each with a rhombic profile in the spanwise direction and both emanating from a single apex. This simple two-body arrangement could conceivably be used as two stores, either embedded within a wing or mounted below a wing, or as auxiliary bodies wherein the upper halves could be used as stores and the lower halves for bomb or missile purposes. The zero-lift wave drag of the system is evaluated herein by means of linearized supersonic flow theory for the entire supersonic speed range. Corresponding calculations for the case of two parallel winglike surfaces with the same cross-sectional shapes as the canted arrangement are included. Consideration is also given to the pressures acting on the blunt bases of both configurations.

LIST OF SYMBOLS

x,y,z	Cartesian coordinates
z_B	z-coordinate defining airfoil section
ξ,η	Cartesian coordinates of source points
V	free-stream or flight velocity
ρ	density of air
Δp	pressure increment
q	dynamic pressure, $\frac{1}{2}\rho V^2$
M	Mach number

β	Mach number parameter, $\sqrt{M^2 - 1}$
ϕ	disturbance-velocity potential
λ	slope of surface (taken in stream direction)
Λ	leading-edge sweepback of body (figs. 1 and 3)
Λ_W	leading-edge sweepback of wing in which canted arrangement is embedded (fig. 1)
θ	inclination of inner edge for the canted arrangement (positive)
k	slope of ridge line, $\frac{1}{2}(\tan\theta + \cot\Lambda)$
c_{max}	maximum chord
t_{max}	maximum thickness
S,A	plan-form area and aspect ratio, respectively (For the canted arrangement, the area includes the cutout inner portion but excludes any wing area exterior to the body leading edge so that $S = (c_{max})^2\cot\Lambda$ and $A = 4\cot\Lambda$ (fig. 1))
S_W,A_W	plan-form area and aspect ratio, respectively, of a delta wing in which the canted arrangement is assumed to be embedded ($S_W = (c_{max})^2\cot\Lambda_W$ and $A_W = 4\cot\Lambda_W$ (fig. 1))
C_D	wave-drag coefficient, $\frac{\text{Wave drag}}{qS}$
C_D'	wave-drag coefficient, $\frac{\text{Wave drag}}{qS_W}$
R	region of integration
V_B	volume of body
l	distance between apexes for the parallel arrangement
s	semispan of one body for the parallel arrangement
$F_1,F_2,\ldots F_8$	functions used in appendix A for summarizing expressions for velocity potentials

Subscripts:

1,2	used as subscripts on λ to denote specific slopes
1,2,3,4	used as subscripts on ϕ to denote the four basic potentials for the canted arrangement
1A,1B,1C,2A,2B	used as subscripts on ϕ to denote special forms of ϕ_1 and ϕ_2
base int	base interference

ANALYSIS

The analysis is based on supersonic thin-airfoil theory and on the assumptions of small disturbances and a constant velocity of sound throughout the fluid. These assumptions lead to the linearized equation for the velocity potential ϕ:

$$(1 - M^2)\phi_{xx} + \phi_{yy} + \phi_{zz} = 0 \tag{1}$$

where M is the Mach number of the flow and the derivatives are taken with respect to the variables x, y, and z of the Cartesian coordinate system. The general expression for the linearized perturbation-velocity potential in space due to a distribution of source and sink singularities in the $z = 0$ plane is (see refs. 2 and 3)

$$\phi(x,y,z) = -\frac{V}{\pi}\iint_R \frac{\lambda(\xi,\eta)d\xi\ d\eta}{\sqrt{(x - \xi)^2 - \beta^2(y - \eta)^2 - \beta^2 z^2}} \tag{2}$$

where x, y, and z are the coordinates of the field point (that is, the point at which the potential is desired) and ξ and η are the coordinates (analogous to x and y) of the singularities. The function $\lambda(\xi,\eta)$ represents the particular distribution of singularities and is, of course, dependent upon the boundary conditions imposed. For the case of wing thickness distributions that are amenable to thin-airfoil-theory calculations, the source-sink distribution function is related to the particular thickness distribution involved and is given as

$$\lambda(\xi,\eta) = \left[\frac{\partial}{\partial\xi} z_B(\xi,\eta)\right]_{z_B=0} \tag{3}$$

The integration indicated in equation (2) is performed over the region R that is enclosed by the traces in the $z = 0$ plane of the Mach forecone emanating from the point (x,y,z) and by the wing plan-form boundaries. Inasmuch as the present problem is concerned with the drag and hence the surface conditions, consistent linearization also requires the potential to be evaluated in the $z = 0$ plane. Thus, the applicable form of equation (2) becomes

$$\phi(x,y) = -\frac{V}{\pi}\iint_R \frac{\frac{\partial}{\partial\xi} z_B(\xi,\eta)}{\sqrt{(x-\xi)^2 - \beta^2(y-\eta)^2}}\, d\xi\, d\eta \tag{4}$$

The parameter β equals $\sqrt{M^2 - 1}$ and its reciprocal $1/\beta$ is the slope (absolute value) of the Mach lines.

Calculation of the wave-drag coefficient involves an integration of the tangential components of surface pressure which are in turn related to the x-derivative of the velocity potential; that is,

$$\begin{aligned} C_D &= \frac{2}{S}\iint_S \frac{\Delta p}{q}\lambda(x,y)dx\, dy \\ &= -\frac{4}{SV}\iint_S \frac{\partial\phi(x,y)}{\partial x}\lambda(x,y)dx\, dy \end{aligned} \tag{5}$$

where S is the plan-form area and the quantity $\frac{\Delta p}{q} = -\frac{2}{V}\frac{\partial\phi(x,y)}{\partial x}$.

The particular thickness distribution in the present problem allows an additional simplification. Inasmuch as the quantity $\lambda(x,y)$ is a constant value over any one region of a wedge-type surface, equation (5) may be expressed simply in terms of the potential by performing an integration with respect to x; that is,

$$C_D = -\frac{4}{SV}\int_b \lambda\phi(x,y)\Big|_{L.E.}^{T.E.} dy \tag{6}$$

where the symbol b denotes that the y-integration is performed over the span. It should be noted, however, that the expression for $\lambda\phi(x,y)$ will generally be different for each wedge region and, therefore, the evaluation between the leading edge and trailing edge as required in the integrand of equation (6) must be taken in finite steps. The solution to the problem consists primarily of calculating the potential for the various surface regions by use of equation (4) and then calculating the drag coefficient by means of equation (6).

Consider now the wing-type arrangement in detail (fig. 1). Four basic potentials ϕ_1, ϕ_2, ϕ_3, and ϕ_4 are required in order to determine the wave drag for the entire supersonic range of Mach numbers; the areas of integration for each of these are indicated in figure 2. In addition, ϕ_1 and ϕ_2 assume different forms for various conditions. A complete summary of the cases treated, mathematical conditions involved, and the appropriate forms of the potentials is given in table I. Before the potentials are evaluated as indicated by equation (4), appropriate expressions for the slopes $\frac{\partial}{\partial\xi} z_B(\xi,\eta)$ must be obtained. For the outboard panels, the slope is found to be

$$\frac{\partial}{\partial\xi} z_B(\xi,\eta) \equiv \lambda_1 = \frac{t_{max}/c_{max}}{1 - (\tan\Lambda)(\tan\theta)} \tag{7}$$

and, for the inboard panels,

$$\frac{\partial}{\partial\xi} z_B(\xi,\eta) \equiv \lambda_2 = -\frac{(\tan\Lambda)(\tan\theta)t_{max}/c_{max}}{1 - (\tan\Lambda)(\tan\theta)} \tag{8}$$

The limits of integration imposed by region R are readily obtained from the information given in figure 2. Expressions for each of the potentials obtained as a result of performing the mathematical operations indicated in equation (4) are presented in appendix A. In accordance with equation (6) the wave-drag coefficient may now be calculated; the resultant expressions are rather lengthy and are presented in appendix B. As a convenience to the reader and as an aid in performing other calculations involving similar integrals, evaluations of some specific indefinite integrals that appear frequently in the analysis herein are given in appendix C.

Wave-drag calculations analogous to those for the canted arrangement were carried out for the case of two parallel bodies separated from each other by an arbitrary distance l (see fig. 3). The mathematical details of obtaining the potentials and so forth are omitted herein; only the required potential expressions and final drag equations are presented in appendix D. It might be noted, however, that the procedures used to obtain these expressions are identical to those utilized for the apex-adjoining arrangement, although much less effort is involved. For example, only two basic potentials are required and the slopes of both the inboard and outboard panels are the same. Furthermore, the work of reference 3 can be used to determine the potentials and wave drag at all supersonic Mach numbers for the case where no interference effects are present.

RESULTS AND DISCUSSION

As indicated in the analysis, closed-form formulas are presented in the appendixes for the complete Mach number range. These formulas enable the drag coefficient for any given plan-form arrangement to be obtained readily by straightforward numerical computation. Therefore, rather than attempting to summarize all possible cases by means of plotting series of design charts, the present paper emphasizes only those salient points that are borne out by the detailed calculations.

The obvious question is whether there is any possible advantage drag-wise in canting the stores or winglike surfaces as indicated. The introduction of a finite value of θ, that is, opening the two panels of the twin-wedge arrangement relative to one another, gives rise to two effects which influence the resultant wave drag. From purely geometric considerations, it is seen that for a given leading-edge sweepback and a constant thickness-chord ratio an increase in the angle θ results in an increase of surface slopes in the stream direction. The trend toward higher slopes is even more pronounced if, instead, the thickness-chord ratio is allowed to vary and the condition of constant volume is imposed. Inasmuch as the supersonic wave drag at zero lift is dependent on the square of the magnitude of such slopes, the effect on the drag is adverse; that is, the drag is increased at all Mach numbers. Canting the two panels, however, also changes the pressure distribution and, since both positive and negative pressures are induced in the field, an assessment of this interference effect is required to determine the net change in the wave-drag coefficient.

Consider the case of $\theta = 0$ wherein the arrangement becomes simply a delta wing with a lateral cross section composed of two diamonds. For this limiting case, the importance and magnitude of the increased-slope effect may be assessed directly by means of comparing the drag with that obtained for the more conventional wing with a lateral cross section composed of a single diamond (equations given in appendix B). The wave-drag coefficients

for both cases are plotted against the aspect-ratio—Mach number parameter $A\beta$ in figure 4. The two configurations have, for a given value of maximum thickness-chord ratio, the same volume and longitudinal distribution of cross-sectional area and the same maximum thickness at each cross section. The main difference is, of course, in the distribution of thickness. The comparison indicates two results which are to be expected in view of previously published wave-drag analyses: First, higher drag values are obtained for the "twin-wedge" case throughout the supersonic speed range (the effective slopes in the stream direction are much higher for this case and hence the drag is correspondingly higher) and, second, this increased-drag effect is more pronounced at the higher Mach numbers (where the leading edge is supersonic). As an interesting sidelight, it might be noted that, inasmuch as the longitudinal distributions of cross-sectional areas are the same for both configurations, application of the "transonic area rule" would yield the same drag coefficient for both cases. Thus, the differences in the ordinates of the two curves give a direct measurement of the degree of inaccuracy involved when this rule is applied to the supersonic speed range.

As might be suggested from consideration of figure 4, the lower supersonic range (where the leading edge is substantially subsonic) appears to be the logical range in which to anticipate net drag reduction as a result of canting the two surfaces. Detailed calculations based on the equations given in appendix B and covering the complete supersonic speed range substantiate this expectation - only in the lower supersonic speed range and for relatively small opening angles is the interference effect sufficiently large to overbalance the adverse drag effect due to the higher local streamwise slopes. At the higher Mach numbers where the leading edge approaches the sonic condition or is supersonic, the wave drag for the canted arrangement is always higher. Figure 5 presents some of the calculations which illustrate these results for the lower supersonic speed range and includes for comparison purposes the uncanted arrangement (that is, $\beta \tan \theta = 0$) previously shown in figure 4.

The results of figure 5 are directly applicable to cases for which the maximum thickness-chord ratio is constant. The curves may be replotted in terms of constant volume or for any other geometric consideration by introducing the appropriate multiplicative factors for each point. Consider, for example, the condition of constant volume; the volume V_B enclosed by both surfaces is given by the expression

$$\left.\begin{aligned} V_B &= \frac{t_{max}\left(c_{max}\right)^2}{3}(\cot \Lambda - \tan \theta) \\ \text{or} \qquad \frac{3\beta V_B}{\left(c_{max}\right)^3} &= \frac{t_{max}}{c_{max}}(\beta \cot \Lambda - \beta \tan \theta) \end{aligned}\right\} \tag{9}$$

and the maximum thickness-chord ratio by

$$\frac{t_{max}}{c_{max}} = \frac{3\beta V_B/(c_{max})^3}{\beta \cot \Lambda - \beta \tan \theta} \tag{10}$$

The wave-drag coefficient given in figure 5 is based on the planform area S (which includes the cutout portion) and is represented as

$$\beta C_D = \left(\frac{t_{max}}{c_{max}}\right)^2 f(\beta \cot \Lambda, \beta \tan \theta) \tag{11}$$

It is readily apparent from equation (9) that, for a fixed overall length, the volume may be maintained constant by either adjusting any two or all three of the parameters Λ, θ, and $\frac{t_{max}}{c_{max}}$. Thus, for a given volume condition, it is desirable to base the wave-drag coefficient on an area which is completely independent of the canted-body geometry so that a true indication of the drag itself may be obtained. A corresponding drag coefficient C_D' based on the area S_W may then be written as

$$\left(\beta A_W\right)\beta C_D' = \left(\frac{t_{max}}{c_{max}}\right)^2 (4\beta \cot \Lambda)\beta C_D \tag{12}$$

where S_W and A_W are the area and aspect ratio, respectively, of a delta wing in which the canted body is assumed to be embedded. For given values of the parameters $\beta \tan \theta$ and $\beta \cot \Lambda$, equation (10) gives the specific thickness ratio required to maintain the desired volume. Equation (11) in conjunction with figure 5 determines the drag coefficient βC_D, and then equation (12) may be used to plot results for the constant-volume condition.

Figure 6 presents results obtained for a specific value of the volume parameter $\frac{3\beta V_B}{(c_{max})^3} = 0.02$. As previously discussed, the ordinate $\left(\beta A_W\right)\left(\beta C_D'\right)$ of figure 6 gives a direct measurement of the drag itself since A_W and S_W (area used for nondimensionalizing C_D') are independent of the canted-body geometry and, therefore, any plotted point in figure 6 may be legitimately compared with any other plotted point to determine whether the drag is decreased or increased when geometry parameters are changed in such a way as to maintain constant volume.

The conclusions to be drawn from figure 6 are as follows: For a given overall length and a given Mach number (constant β), it is possible

to redistribute a given volume in a manner practical for store purposes and obtain drag reduction by canting the bodies slightly. (Compare, for example, the values indicated by the filled-in circles.) If, in addition to a constant volume a constant maximum thickness-chord ratio is desired, then canting the bodies will always result in increased drag (follow the dashed lines). Similarly, if in addition to constant volume a constant sweepback angle Λ is desired, then canting the bodies will result in increased drag (follow vertical lines). Figure 6 is, of course, directly applicable to the volume parameter $\frac{3\beta V_B}{(c_{max})^3} = 0.02$, but the results are indicative of those found for other values of the volume parameter. Figure 5 in conjunction with equations (10), (11), and (12) may be used as just outlined to obtain detailed curves for other volume conditions and thickness ratios.

Calculations of the supersonic wave drag for the parallel-body arrangement consisting of two surfaces of delta plan form, each with a simple wedge profile and with parallel axes of symmetry (see fig. 3), are presented in figure 7. The interesting point to be noted is that when the two surfaces are in the interference fields of each other the resulting interference drag is additive; that is, the drag of the arrangement is least when the combination of Mach number and lateral displacement of the two apexes is such that the disturbance field of one surface does not influence the drag of the other surface. This result is expected inasmuch as the pressure due to a single wedge is the same in sign over the wedge surface and in the field beyond the wedge; therefore, the introduction of a similar wedge into the field (such as in the present case) will result in additional drag of the same sign as the pressure drag of the original body.

Inasmuch as both the canted and parallel arrangements treated in the present paper have blunt bases, it is advisable to point out that the drag calculations discussed thus far do not take into account either the basic base drag or the interference-drag contribution resulting from the pressure field generated by one panel acting on the blunt base of the opposite panel. Actually, this interference effect gives rise to a negative drag, or thrust, and could conceivably be of the same order of magnitude as the interference contribution previously considered.

In order to assess the importance of the base-drag-interference contribution, the interference pressures acting on the base have been derived for both arrangements of bodies and are presented in appendix E. Specifically, the formulas give the interference-pressure coefficient $\left(\frac{\Delta p}{q}\right)_{\text{base int}}$ acting along the base line in the plane of symmetry, that is, $x = c_{max}$ and

$z = 0$. The formulas were obtained by utilizing equation (4) to find the interference velocity potential (changing the region R to include only that portion bounded by the Mach trace and plan-form boundary of the opposite or interfering body), differentiating to find the pressure coefficient $\left(\frac{\Delta p}{q} = -\frac{2}{V}\frac{\partial\phi(x,y)}{\partial x}\right)$, and then evaluating the result along the line $x = c_{max}$.

Numerical calculations for this base interference effect were carried out for the parallel arrangement of bodies to ascertain whether the favorable drag increment would counterbalance the increase in drag previously found and indicated in figure 7. A rough estimate of the decrement in drag was obtained by first plotting the variation in pressure acting on the base (illustrated in fig. 8 for a distance parameter $\frac{l}{s} = 3.0$ and several Mach number-sweepback arrangements) obtained by use of the formulas in appendix E, and then essentially integrating this pressure distribution over the base area affected by the interference flow. The decremental drag coefficient ΔC_D as found by this crude approach is believed to give a reasonable approximation to the magnitude of the base interference effect. Values of the decrement $\frac{\beta\,\Delta C_D}{\left(t_{max}/c_{max}\right)^2}$ found by the above-outlined procedure for the cases presented in figure 8 were 0.13, 0.14, and 0.013 for the parameter $\beta \cot \Lambda = 0.10$, 0.25, and 0.40, respectively. Subtraction of these drag decrements from the corresponding ordinates of figure 7 result in values that fall beneath the "no interference, $\frac{l}{s} \rightarrow \infty$" curve presented therein. Additional calculations covering the range of sweepback, Mach number, and distance-between-bodies parameter indicated the same result, namely, that the base interference effect was generally of sufficient magnitude to overbalance the adverse interference effect previously found (see fig. 7) and, thus, the overall interference effect on the drag was favorable. Analogous calculations for the canted-body arrangement can be carried out with the use of the appropriate formulas of appendix E and the procedure previously indicated for the parallel arrangement of bodies. It is apparent that the magnitude of the opening angle is a critical parameter with regard to the net interference-drag contribution.

CONCLUDING REMARKS

An analysis, based on the linearized thin-airfoil theory for supersonic speeds, of the wave drag at zero lift has been carried out for a simple two-body arrangement consisting of two wedgelike surfaces, each with a rhombic lateral cross section and emanating from a common apex.

Such an arrangement could be used as two stores, either embedded within or mounted below a wing, or as auxiliary bodies wherein the upper halves could be used as stores and the lower halves for bomb or missile purposes. The complete range of supersonic Mach numbers has been considered and it was found that by canting or orienting the axes of the bodies relative to each other a given volume may be redistributed in a manner which enables the wave drag to be reduced at the lower supersonic speeds. For purposes of comparison, analogous drag calculations for the case of two parallel winglike bodies with the same cross-sectional shapes as the canted arrangement have been included. Some consideration has also been given to the problem of estimating the favorable (dragwise) interference pressures acting on the blunt bases of both configurations. In the case of the parallel bodies for which calculations were made, this base effect seemed more than sufficient to cancel the unfavorable interference on the forward part of the configuration.

Langley Aeronautical Laboratory,
National Advisory Committee for Aeronautics,
Langley Field, Va., July 18, 1957.

APPENDIX A

SUMMARY OF VELOCITY POTENTIALS

FOR CANTED ARRANGEMENT

The required velocity potentials for the canted arrangement of bodies (see table I) may be conveniently expressed in the following form:

$$\phi_{1A} = F_1 + F_2 + F_4$$

$$\phi_{1B} = F_1 + F_3 + F_4$$

$$\phi_{1C} = F_5 + F_2 + F_4$$

$$\phi_{2A} = F_6 + F_2 + F_4$$

$$\phi_{2B} = F_6 + F_3 + F_4$$

$$\phi_3 = F_7$$

$$\phi_4 = F_7 + F_8$$

where the functions F_1 to F_8 are defined as follows:

$$F_1 = \frac{V(\lambda_1 - \lambda_2)}{\pi\sqrt{1 - \beta^2k^2}}\left[(kx - y)\cosh^{-1}\frac{x - \beta^2ky}{\beta(kx - y)} + (kx + y)\cosh^{-1}\frac{x + \beta^2ky}{\beta(kx + y)}\right]$$

$$F_2 = \frac{-V\lambda_1}{\pi\sqrt{\beta^2 - \tan^2\Lambda}}\left[(x + y\tan\Lambda)\cos^{-1}\frac{x\tan\Lambda + \beta^2y}{\beta(y\tan\Lambda + x)} + \right.$$

$$\left.(x - y\tan\Lambda)\cos^{-1}\frac{x\tan\Lambda - \beta^2y}{\beta(x - y\tan\Lambda)}\right]$$

$$F_3 = \frac{-V\lambda_1}{\pi\sqrt{\tan^2 \Lambda - \beta^2}}\left[(x + y \tan \Lambda)\cosh^{-1} \frac{x \tan \Lambda + \beta^2 y}{\beta(x + y \tan \Lambda)} + \right.$$

$$\left.(x - y \tan \Lambda)\cosh^{-1} \frac{x \tan \Lambda - \beta^2 y}{\beta(x - y \tan \Lambda)}\right]$$

$$F_4 = \frac{V\lambda_2}{\pi\sqrt{\cot^2 \theta - \beta^2}}\left[(x - y \cot \theta)\cosh^{-1} \frac{x \cot \theta - \beta^2 y}{\beta(y \cot \theta - x)} + \right.$$

$$\left.(x + y \cot \theta)\cosh^{-1} \frac{x \cot \theta + \beta^2 y}{\beta(y \cot \theta + x)}\right]$$

$$F_5 = \frac{V(\lambda_1 - \lambda_2)}{\pi\sqrt{\beta^2 k^2 - 1}}\left[(kx - y)\cos^{-1} \frac{x - \beta^2 ky}{\beta(kx - y)} + (kx + y)\cos^{-1} \frac{x + \beta^2 ky}{\beta(kx + y)}\right]$$

$$F_6 = \frac{V(\lambda_1 - \lambda_2)}{\pi\sqrt{1 - \beta^2 k^2}}\left[(kx - y)\cosh^{-1} \frac{x - \beta^2 ky}{\beta(y - kx)} + (kx + y)\cosh^{-1} \frac{x + \beta^2 ky}{\beta(kx + y)}\right]$$

$$F_7 = \frac{V\lambda_1}{\beta^2\sqrt{\cot^2 \Lambda - 1}}(y - x \cot \Lambda)$$

$$F_8 = \frac{V(\lambda_1 - \lambda_2)}{\sqrt{\beta^2 k^2 - 1}}(kx - y)$$

APPENDIX B

SUMMARY OF EQUATIONS FOR THE WAVE-DRAG COEFFICIENT OF THE CANTED ARRANGEMENT

For the case wherein all the edges are subsonic, that is, $\beta \cot \Lambda < 1$, the formula for the wave-drag coefficient is

$$
\begin{aligned}
\frac{\beta C_D}{(t_{max}/c_{max})^2} = -\frac{2}{\pi\beta \cot \Lambda}\Bigg\{ & \frac{(\beta \cot \Lambda + \beta \tan \theta)^2}{(\beta \cot \Lambda - \beta \tan \theta)\sqrt{4 - (\beta \tan \theta + \beta \cot \Lambda)^2}}\Bigg[\beta \cot \Lambda \cosh^{-1} \frac{2 - (\beta^2 \cot^2 \Lambda + \beta \cot \Lambda\, \beta \tan \theta)}{\beta \cot \Lambda - \beta \tan \theta} + \\
& \frac{\beta \cot \Lambda(\beta \tan \theta + 3\beta \cot \Lambda)}{\beta \cot \Lambda - \beta \tan \theta} \cosh^{-1} \frac{2 + (\beta^2 \cot^2 \Lambda + \beta \tan \theta\, \beta \cot \Lambda)}{\beta \tan \theta + 3\beta \cot \Lambda} - \beta \tan \theta \cosh^{-1} \frac{2 - (\beta^2 \tan^2 \theta + \beta \tan \theta\, \beta \cot \Lambda)}{\beta \cot \Lambda - \beta \tan \theta} + \\
& \frac{\beta \tan \theta(3\beta \tan \theta + \beta \cot \Lambda)}{\beta \cot \Lambda - \beta \tan \theta} \cosh^{-1} \frac{2 + (\beta^2 \tan^2 \theta + \beta \tan \theta\, \beta \cot \Lambda)}{\beta \cot \Lambda + 3\beta \tan \theta} - \frac{2(\beta \cot \Lambda + \beta \tan \theta)^2}{\beta \cot \Lambda - \beta \tan \theta} \cosh^{-1} \frac{4 + (\beta \tan \theta + \beta \cot \Lambda)^2}{4(\beta \tan \theta + \beta \cot \Lambda)}\Bigg] + \\
& \frac{\beta^2 \cot^2 \Lambda}{(\beta \cot \Lambda - \beta \tan \theta)\sqrt{1 - \beta^2 \cot^2 \Lambda}}\Bigg[\frac{(\beta \cot \Lambda + \beta \tan \theta)(3\beta \cot \Lambda + \beta \tan \theta)}{\beta \cot \Lambda - \beta \tan \theta} \cosh^{-1} \frac{2 + (\beta^2 \cot^2 \Lambda + \beta \tan \theta\, \beta \cot \Lambda)}{\beta \tan \theta + 3\beta \cot \Lambda} - \\
& (\beta \cot \Lambda + \beta \tan \theta)\cosh^{-1} \frac{2 - (\beta^2 \cot^2 \Lambda + \beta \tan \theta\, \beta \cot \Lambda)}{\beta \cot \Lambda - \beta \tan \theta} + 2\beta \tan \theta \cosh^{-1} \frac{1 - \beta \tan \theta\, \beta \cot \Lambda}{\beta \cot \Lambda - \beta \tan \theta} - \\
& \frac{2\beta \tan \theta(\beta \tan \theta + \beta \cot \Lambda)}{\beta \cot \Lambda - \beta \tan \theta} \cosh^{-1} \frac{1 + \beta \tan \theta\, \beta \cot \Lambda}{\beta \cot \Lambda + \beta \tan \theta} - \frac{4\beta^2 \cot^2 \Lambda}{\beta \cot \Lambda - \beta \tan \theta} \cosh^{-1} \frac{1 + \beta^2 \cot^2 \Lambda}{2\beta \cot \Lambda}\Bigg] + \\
& \frac{\beta^2 \tan^2 \theta}{(\beta \cot \Lambda - \beta \tan \theta)\sqrt{1 - \beta^2 \tan^2 \theta}}\Bigg[(\beta \cot \Lambda + \beta \tan \theta)\cosh^{-1} \frac{2 - (\beta^2 \tan^2 \theta + \beta \cot \Lambda\, \beta \tan \theta)}{\beta \cot \Lambda - \beta \tan \theta} +
\end{aligned}
$$

(equation continued on next page)

$$\frac{(\beta \cot \Lambda + \beta \tan \theta)(\beta \cot \Lambda + 3\beta \tan \theta)}{\beta \cot \Lambda - \beta \tan \theta} \cosh^{-1} \frac{2 + (\beta^2 \tan^2 \theta + \beta \cot \Lambda \beta \tan \theta)}{\beta \cot \Lambda + 3\beta \tan \theta} - 2\beta \cot \Lambda \cosh^{-1} \frac{1 - \beta \tan \theta \beta \cot \Lambda}{\beta \cot \Lambda - \beta \tan \theta} -$$

$$\frac{2\beta \cot \Lambda(\beta \cot \Lambda + \beta \tan \theta)}{\beta \cot \Lambda - \beta \tan \theta} \cosh^{-1} \frac{1 + \beta \tan \theta \beta \cot \Lambda}{\beta \cot \Lambda + \beta \tan \theta} - \frac{4\beta^2 \tan^2 \theta}{\beta \cot \Lambda - \beta \tan \theta} \cosh^{-1} \frac{1 + \beta^2 \tan^2 \theta}{2\beta \tan \theta}\Bigg] +$$

$$2\left[\beta \cot \Lambda \cos^{-1} \beta \cot \Lambda + \beta \tan \theta \cos^{-1} \beta \tan \theta - (\beta \cot \Lambda + \beta \tan \theta)\cos^{-1} \tfrac{1}{2}(\beta \tan \theta + \beta \cot \Lambda)\right]\Bigg\} \tag{B1}$$

As the speed range progresses to the point where the leading edge becomes sonic, that is, $\beta \cot \Lambda = 1$, equation (B1) reduces to

$$\frac{\beta C_D}{(t_{max}/c_{max})^2} = -\frac{2}{\pi}\Bigg\{\frac{(1 + \beta \tan \theta)^2}{(1 - \beta \tan \theta)\sqrt{4 - (\beta \tan \theta + 1)^2}}\Bigg[-\beta \tan \theta \cosh^{-1}(2 + \beta \tan \theta) + \frac{\beta \tan \theta(3\beta \tan \theta + 1)}{1 - \beta \tan \theta} \cosh^{-1} \frac{2 + \beta \tan \theta + \beta^2 \tan^2 \theta}{1 + 3\beta \tan \theta} -$$

$$\frac{2(1 + \beta \tan \theta)^2}{1 - \beta \tan \theta} \cosh^{-1} \frac{4 + (\beta \tan \theta + 1)^2}{4(\beta \tan \theta + 1)}\Bigg] + \frac{\beta^2 \tan^2 \theta}{(1 - \beta \tan \theta)\sqrt{1 - \beta^2 \tan^2 \theta}}\Bigg[(1 + \beta \tan \theta)\cosh^{-1}(2 + \beta \tan \theta) +$$

$$\frac{(1 + \beta \tan \theta)(1 + 3\beta \tan \theta)}{1 - \beta \tan \theta} \cosh^{-1} \frac{2 + \beta \tan \theta + \beta^2 \tan^2 \theta}{1 + 3\beta \tan \theta} - \frac{4\beta^2 \tan^2 \theta}{1 - \beta \tan \theta} \cosh^{-1} \frac{1 + \beta^2 \tan^2 \theta}{2\beta \tan \theta}\Bigg] +$$

$$2\left[\beta \tan \theta \cos^{-1} \beta \tan \theta - (1 + \beta \tan \theta)\cos^{-1} \tfrac{1}{2}(1 + \beta \tan \theta)\right]\Bigg\} \tag{B2}$$

For the condition in which the leading edge is supersonic but the remaining edges are subsonic, that is, $\beta \cot \Lambda > 1$, $\beta\left(\frac{\tan \theta + \cot \Lambda}{2}\right) < 1$, the equation for the wave-drag coefficient is

$$\frac{\beta C_D}{(t_{max}/c_{max})^2} = -\frac{2}{\pi\beta \cot \Lambda}\left\{\frac{1}{\sqrt{4 - (\beta \tan \theta + \beta \cot \Lambda)^2}}\left[\frac{\beta \tan \theta(\beta \cot \Lambda + \beta \tan \theta)^2}{\beta \tan \theta - \beta \cot \Lambda} \cosh^{-1} \frac{2 - \beta \tan \theta(\beta \cot \Lambda + \beta \tan \theta)}{\beta \cot \Lambda - \beta \tan \theta} + \right.\right.$$

$$\frac{\beta \tan \theta(\beta \cot \Lambda + \beta \tan \theta)(3\beta^2 \tan^2 \theta + 4\beta \tan \theta\ \beta \cot \Lambda + \beta^2 \cot^2 \Lambda)}{(\beta \cot \Lambda - \beta \tan \theta)^2} \cosh^{-1} \frac{2 + \beta \tan \theta(\beta \cot \Lambda + \beta \tan \theta)}{\beta \cot \Lambda + 3\beta \tan \theta} -$$

$$\left.\frac{2(\beta \cot \Lambda + \beta \tan \theta)^4}{(\beta \cot \Lambda - \beta \tan \theta)^2} \cosh^{-1} \frac{4 + (\beta \cot \Lambda + \beta \tan \theta)^2}{4(\beta \cot \Lambda + \beta \tan \theta)}\right] + \frac{\beta^2 \cot^2 \Lambda}{\sqrt{\beta^2 \cot^2 \Lambda - 1}}\left[\frac{\beta^2 \tan^2 \theta - \beta^2 \cot^2 \Lambda}{(\beta \cot \Lambda - \beta \tan \theta)^2} \cos^{-1} \frac{2 - \beta \cot \Lambda(\beta \cot \Lambda + \beta \tan \theta)}{\beta \cot \Lambda - \beta \tan \theta} + \right.$$

$$\frac{(\beta \cot \Lambda + \beta \tan \theta)(3\beta \cot \Lambda + \beta \tan \theta)}{(\beta \cot \Lambda - \beta \tan \theta)^2} \cos^{-1} \frac{2 + \beta \cot \Lambda(\beta \cot \Lambda + \beta \tan \theta)}{3\beta \cot \Lambda + \beta \tan \theta} + \frac{2\beta \tan \theta}{\beta \cot \Lambda - \beta \tan \theta} \cos^{-1} \frac{1 - \beta \cot \Lambda\ \beta \tan \theta}{\beta \cot \Lambda - \beta \tan \theta} -$$

$$\left.\frac{2\beta \tan \theta(\beta \cot \Lambda + \beta \tan \theta)}{(\beta \cot \Lambda - \beta \tan \theta)^2} \cos^{-1} \frac{1 + \beta \cot \Lambda\ \beta \tan \theta}{\beta \cot \Lambda + \beta \tan \theta}\right] + \frac{\beta^2 \tan^2 \theta}{\sqrt{1 - \beta^2 \tan^2 \theta}}\left[\frac{\beta \cot \Lambda + \beta \tan \theta}{\beta \cot \Lambda - \beta \tan \theta} \cosh^{-1} \frac{2 - \beta \tan \theta(\beta \cot \Lambda + \beta \tan \theta)}{\beta \cot \Lambda - \beta \tan \theta} + \right.$$

$$\left.\frac{(\beta \cot \Lambda + \beta \tan \theta)(\beta \cot \Lambda + 3\beta \tan \theta)}{(\beta \cot \Lambda - \beta \tan \theta)^2} \cosh^{-1} \frac{2 + \beta \tan \theta(\beta \cot \Lambda + \beta \tan \theta)}{\beta \cot \Lambda + 3\beta \tan \theta} - \frac{4\beta^2 \tan^2 \theta}{(\beta \cot \Lambda - \beta \tan \theta)^2} \cosh^{-1} \frac{1 + \beta^2 \tan^2 \theta}{2\beta \tan \theta}\right] -$$

$$\left.2(\beta \cot \Lambda + \beta \tan \theta)\cos^{-1} \frac{\beta \cot \Lambda + \beta \tan \theta}{2} + 2\beta \tan \theta \cos^{-1} \beta \tan \theta\right\} \tag{B3}$$

When the ridge line becomes sonic, that is, $\beta\left(\frac{\tan \theta + \cot \Lambda}{2}\right) = 1$, equation (B3) reduces to

$$\frac{\beta C_D}{(t_{max}/c_{max})^2} = -\frac{2}{\pi\beta \cot \Lambda}\left\{\frac{\beta^2 \cot^2 \Lambda}{\sqrt{\beta^2 \cot^2 \Lambda - 1}}\left[\frac{\pi}{1 - \beta \cot \Lambda} + \frac{2 - \beta \cot \Lambda}{\beta \cot \Lambda - 1} \cos^{-1} \frac{\beta \cot \Lambda - 1}{2} + \frac{\beta \cot \Lambda - 2}{(\beta \cot \Lambda - 1)^2} \cos^{-1} \frac{1 + 2\beta \cot \Lambda - \beta^2 \cot^2 \Lambda}{2}\right] -\right.$$

$$\left.\frac{(2 - \beta \cot \Lambda)^4}{(\beta \cot \Lambda - 1)^2\sqrt{-3 + 4\beta \cot \Lambda - \beta^2 \cot^2 \Lambda}} \cosh^{-1} \frac{3 - 4\beta \cot \Lambda + \beta^2 \cot^2 \Lambda}{2(2 - \beta \cot \Lambda)} + 2(2 - \beta \cot \Lambda)\cos^{-1}(2 - \beta \cot \Lambda)\right\} \tag{B4}$$

For the condition in which both the leading edge and ridge lines are supersonic but the innermost edge is subsonic, that is, $\beta\left(\frac{\tan\theta + \cot\Lambda}{2}\right) > 1$, $\beta \tan\theta < 1$, the formula for the wave-drag coefficient is

$$
\begin{aligned}
\frac{\beta C_D}{\left(t_{max}/c_{max}\right)^2} = -\frac{2}{\pi\beta\cot\Lambda}\Bigg(&\frac{\pi\beta^2\cot^2\Lambda}{2\sqrt{\beta^2\cot^2\Lambda - 1}}\Bigg\{\frac{(\beta\cot\Lambda + \beta\tan\theta)^2}{\beta\cot\Lambda(\beta\tan\theta - \beta\cot\Lambda)} - \\
&\frac{\beta\tan\theta}{\beta\cot\Lambda(\beta\cot\Lambda - \beta\tan\theta)^2}\left[(\beta\tan\theta + \beta\cot\Lambda)(\beta\tan\theta - 3\beta\cot\Lambda) - 4 + 8\beta\cot\Lambda\right] - 1\Bigg\} + \\
&\frac{1}{\sqrt{(\beta\tan\theta + \beta\cot\Lambda)^2 - 4}}\Bigg[\frac{\beta\tan\theta(\beta\cot\Lambda + \beta\tan\theta)^2}{\beta\tan\theta - \beta\cot\Lambda}\cos^{-1}\frac{2 - (\beta^2\tan^2\theta + \beta\tan\theta\,\beta\cot\Lambda)}{\beta\cot\Lambda - \beta\tan\theta} + \\
&\frac{\beta\tan\theta(3\beta\tan\theta + \beta\cot\Lambda)(\beta\tan\theta + \beta\cot\Lambda)^2}{(\beta\cot\Lambda - \beta\tan\theta)^2}\cos^{-1}\frac{2 + (\beta^2\tan^2\theta + \beta\tan\theta\,\beta\cot\Lambda)}{\beta\cot\Lambda + 3\beta\tan\theta} - \\
&\frac{2\beta\tan\theta(\beta\cot\Lambda + \beta\tan\theta)^2}{(\beta\cot\Lambda - \beta\tan\theta)^2}\sqrt{(\beta\tan\theta + \beta\cot\Lambda)^2 - 4}\cos^{-1}\beta\tan\theta\Bigg] + \frac{2}{\sqrt{\beta^2\cot^2\Lambda - 1}}\Bigg[\frac{\beta^2\cot^2\Lambda\,\beta\tan\theta}{\beta\cot\Lambda - \beta\tan\theta}\cos^{-1}\frac{1 - \beta\tan\theta\,\beta\cot\Lambda}{\beta\cot\Lambda - \beta\tan\theta} - \\
&\frac{\beta^2\cot^2\Lambda\,\beta\tan\theta(\beta\tan\theta + \beta\cot\Lambda)}{(\beta\cot\Lambda - \beta\tan\theta)^2}\cos^{-1}\frac{1 + \beta\tan\theta\,\beta\cot\Lambda}{\beta\cot\Lambda + \beta\tan\theta} - \frac{\beta\cot\Lambda\,\beta\tan\theta}{(\beta\cot\Lambda - \beta\tan\theta)^2}\pi(1 - \beta\cot\Lambda)^2 + \\
&\frac{2\beta^2\cot^2\Lambda\,\beta\tan\theta}{(\beta\cot\Lambda - \beta\tan\theta)^2}\sqrt{\beta^2\cot^2\Lambda - 1}\cos^{-1}\beta\tan\theta\Bigg] + \frac{4}{\sqrt{1 - \beta^2\tan^2\theta}}\cdot\frac{\beta^4\tan^4\theta}{(\beta\tan\theta - \beta\cot\Lambda)^2}\Bigg(-\cosh^{-1}\frac{1 + \beta^2\tan^2\theta}{2\beta\tan\theta} + \\
&\frac{1}{\beta\tan\theta}\sqrt{1 - \beta^2\tan^2\theta}\cos^{-1}\beta\tan\theta\Bigg)\Bigg)
\end{aligned}
\tag{B5}
$$

When the innermost edge is sonic, that is, $\beta \tan \theta = 1$, equation (B5) reduces to

$$\frac{\beta C_D}{\left(t_{max}/c_{max}\right)^2} = 2\beta \cot \Lambda \left[\frac{1}{\sqrt{\beta^2 \cot^2 \Lambda - 1}} + \frac{(\beta \cot \Lambda + 1)^2}{(\beta \cot \Lambda - 1)\beta^2 \cot^2 \Lambda \sqrt{(\beta \cot \Lambda + 1)^2 - 4}}\right] \tag{B6}$$

For the speed condition where all edges are supersonic, that is, $\beta \tan \theta > 1$, the drag coefficient is given by

$$\frac{\beta C_D}{\left(t_{max}/c_{max}\right)^2} = 2\beta \cot \Lambda \left[\frac{(\beta \tan \theta + \beta \cot \Lambda)^2 \beta \tan \theta}{(\beta^2 \cot^2 \Lambda)(\beta \cot \Lambda - \beta \tan \theta)\sqrt{(\beta \tan \theta + \beta \cot \Lambda)^2 - 4}} + \frac{1}{\sqrt{\beta^2 \cot^2 \Lambda - 1}}\right] \tag{B7}$$

It is to be noted that the drag coefficient given by equations (B1) to (B7) is based on an area which includes the "cutout" portion; that is, the reference area is that of a delta wing having the same leading-edge sweepback.

For the special case of $\theta = 0$, considerable simplification is introduced into the equations, and the formulas for wave-drag coefficient for this case as well as those for the single-wedge delta used for comparison purposes in figure 4 are summarized in the following table:

Range of $A\beta$	$\dfrac{\beta C_D}{\left(t_{max}/c_{max}\right)^2}$
Canted arrangement, $\theta = 0$	
0	0
$0 < A\beta < 4$	$\dfrac{2A\beta}{\pi\sqrt{64 - A^2\beta^2}}\left(2 \cosh^{-1} \dfrac{A^2\beta^2 + 64}{16A\beta} - 3 \cosh^{-1} \dfrac{A^2\beta^2 + 32}{12A\beta} - \cosh^{-1} \dfrac{32 - A^2\beta^2}{4A\beta}\right) + \dfrac{2A\beta}{\pi\sqrt{16 - A^2\beta^2}}\left(\cosh^{-1} \dfrac{32 - A^2\beta^2}{4A\beta} + 4 \cosh^{-1} \dfrac{A^2\beta^2 + 16}{8A\beta} - 3 \cosh^{-1} \dfrac{A^2\beta^2 + 32}{12A\beta}\right) + \dfrac{4}{\pi}\left(\cos^{-1} \dfrac{A\beta}{8} - \cos^{-1} \dfrac{A\beta}{4}\right)$
$A\beta = 4$	$\dfrac{4}{3}\left(1 + \dfrac{\sqrt{3}}{\pi} \cosh^{-1} \dfrac{5}{4}\right) = 1.84$
$4 < A\beta < 8$	$\dfrac{4A\beta}{\pi}\left(\dfrac{1}{A\beta} \cos^{-1} \dfrac{A\beta}{8} + \dfrac{1}{\sqrt{64 - A^2\beta^2}} \cosh^{-1} \dfrac{A^2\beta^2 + 64}{16A\beta} - \dfrac{3}{2\sqrt{A^2\beta^2 - 16}} \cos^{-1} \dfrac{A^2\beta^2 + 32}{12A\beta} + \dfrac{1}{2\sqrt{A^2\beta^2 - 16}} \cos^{-1} \dfrac{32 - A^2\beta^2}{4A\beta}\right)$
$A\beta \geqq 8$	$\dfrac{2A\beta}{\sqrt{A^2\beta^2 - 16}}$
Single-wedge delta (see ref. 3)	
0	0
$0 < A\beta < 4$	$\dfrac{2}{\pi}\left(\sin^{-1} \dfrac{A\beta}{4} - \dfrac{A\beta}{\sqrt{16 - A^2\beta^2}} \log_e \dfrac{A\beta}{4}\right)$
$A\beta \geqq 4$	1

APPENDIX C

SOME SPECIFIC INTEGRALS OF INTEREST OCCURRING IN THE DRAG ANALYSIS

Consider the indefinite integrals

$$I_1 = \int \cos^{-1} \frac{cy + d}{ay + b}\, dy$$

$$I_2 = \int \cosh^{-1} \frac{cy + d}{ay + b}\, dy$$

$$I_3 = \int y \cos^{-1} \frac{cy + d}{ay + b}\, dy$$

$$I_4 = \int y \cosh^{-1} \frac{cy + d}{ay + b}\, dy$$

where a, b, c, and d are constants subject to the condition that $ay + b > 0$. (Note that this condition is not restrictive inasmuch as the term can always be made positive by reversing signs in both numerator and denominator.)

For $a^2 > c^2$:

$$I_1 = \frac{ay + b}{a} \cos^{-1} \frac{cy + d}{ay + b} + \frac{ad - bc}{a\sqrt{a^2 - c^2}} \cosh^{-1} \frac{y(c^2 - a^2) + cd - ab}{|bc - ad|}^{*}$$

$$I_2 = \frac{ay + b}{a} \cosh^{-1} \frac{cy + d}{ay + b} + \frac{ad - bc}{a\sqrt{a^2 - c^2}} \cos^{-1} \frac{y(c^2 - a^2) + cd - ab}{|bc - ad|}$$

$$I_3 = \frac{a^2y^2 - b^2}{2a^2} \cos^{-1} \frac{cy + d}{ay + b} - \frac{ad - bc}{2a(a^2 - c^2)} \sqrt{-Y} +$$

$$\frac{c(a^2d^2 - b^2c^2) - 2a^2b(ad - bc)}{2a^2(a^2 - c^2)^{3/2}} \cosh^{-1} \frac{y(c^2 - a^2) + (cd - ab)}{|bc - ad|}^{*}$$

$$I_4 = \frac{a^2y^2 - b^2}{2a^2} \cosh^{-1} \frac{cy + d}{ay + b} - \frac{ad - bc}{2a(a^2 - c^2)}\sqrt{Y} +$$

$$\frac{c(a^2d^2 - b^2c^2) - 2a^2b(ad - bc)}{2a^2(a^2 - c^2)^{3/2}} \cos^{-1} \frac{y(c^2 - a^2) + (cd - ab)}{|bc - ad|}$$

For $a^2 < c^2$:

$$I_1 = \frac{ay + b}{a} \cos^{-1} \frac{cy + d}{ay + b} + \frac{ad - bc}{a\sqrt{c^2 - a^2}} \cos^{-1} \frac{y(c^2 - a^2) + (cd - ab)}{|bc - ad|}$$

$$I_2 = \frac{ay + b}{a} \cosh^{-1} \frac{cy + d}{ay + b} + \frac{ad - bc}{a\sqrt{c^2 - a^2}} \cosh^{-1} \frac{y(c^2 - a^2) + (cd - ab)}{|bc - ad|}^{*}$$

$$I_3 = \frac{a^2y^2 - b^2}{2a^2} \cos^{-1} \frac{cy + d}{ay + b} + \frac{ad - bc}{2a(c^2 - a^2)}\sqrt{-Y} -$$

$$\frac{c(a^2d^2 - b^2c^2) - 2a^2b(ad - bc)}{2a^2(c^2 - a^2)^{3/2}} \cos^{-1} \frac{y(c^2 - a^2) + cd - ab}{|bc - ad|}$$

$$I_4 = \frac{a^2y^2 - b^2}{2a^2} \cosh^{-1} \frac{cy + d}{ay + b} + \frac{ad - bc}{2a(c^2 - a^2)}\sqrt{Y} -$$

$$\frac{c(a^2d^2 - b^2c^2) - 2a^2b(ad - bc)}{2a^2(c^2 - a^2)^{3/2}} \cosh^{-1} \frac{y(c^2 - a^2) + cd - ab}{|bc - ad|}^{*}$$

where the quantity $Y = (c^2 - a^2)y^2 + 2(cd - ab)y + d^2 - b^2$ and the asterisk indicates that if the inverse hyperbolic cosine should be required of a negative number $-N$ then the following relationship must be used:

$$\cosh^{-1} (-N) = -\cosh^{-1} N$$

APPENDIX D

SUMMARY OF FORMULAS FOR VELOCITY POTENTIALS AND WAVE DRAG FOR THE PARALLEL ARRANGEMENT

The basic potentials required to evaluate the wave drag of the parallel arrangement of surfaces (see fig. 3) may be obtained for the case of subsonic leading edges involving interference effects by the procedure outlined in the body of the paper. At all supersonic Mach numbers for which the particular region of one surface under consideration is outside the domain of interference from the opposite surface, the potential expressions may be readily reduced from reference 3. For convenience, all the applicable potential expressions are summarized in the following formulas:

Subsonic leading edge; region outside interference field:

$$\phi = \frac{V\left(t_{max}/c_{max}\right)}{2\pi\sqrt{1 - \beta^2 \cot^2 \Lambda}}\left[(y - x \cot \Lambda)\cosh^{-1} \frac{x - y\beta^2 \cot \Lambda}{\beta(x \cot \Lambda - y)} - (y + x \cot \Lambda)\cosh^{-1} \frac{x + y\beta^2 \cot \Lambda}{\beta(x \cot \Lambda + y)}\right] \tag{D1}$$

Subsonic leading edge; region within interference field:

$$\phi = \frac{V\left(t_{max}/c_{max}\right)}{2\pi\sqrt{1 - \beta^2 \cot^2 \Lambda}}\left[(y - x \cot \Lambda)\cosh^{-1} \frac{x - y\beta^2 \cot \Lambda}{\beta(x \cot \Lambda - y)} - (y + x \cot \Lambda)\cosh^{-1} \frac{x + y\beta^2 \cot \Lambda}{\beta(x \cot \Lambda + y)} + (y + l - x \cot \Lambda)\cosh^{-1} \frac{x - (y + l)\beta^2 \cot \Lambda}{\beta(y + l - x \cot \Lambda)} - (y + l + x \cot \Lambda)\cosh^{-1} \frac{x + (y + l)\beta^2 \cot \Lambda}{\beta(y + l + x \cot \Lambda)}\right] \tag{D2}$$

Supersonic leading edge; region outside Mach traces from apex:

$$\phi = \frac{V\left(t_{max}/c_{max}\right)(y - x \cot \Lambda)}{2\sqrt{\beta^2 \cot^2 \Lambda - 1}} \tag{D3}$$

Supersonic leading edge; region within Mach traces from apex:

$$\phi = \frac{V\left(t_{max}/c_{max}\right)}{2\pi\sqrt{\beta^2 \cot^2 \Lambda - 1}}\left[(y - x \cot \Lambda)\cos^{-1} \frac{x - y\beta^2 \cot \Lambda}{\beta(x \cot \Lambda - y)} - (y + x \cot \Lambda)\cos^{-1} \frac{x + y\beta^2 \cot \Lambda}{\beta(x \cot \Lambda + y)}\right] \tag{D4}$$

The formulas for wave-drag coefficient are based on the plan-form area of both surfaces and are given as follows:

For $0 < \beta \cot \Lambda \leqq \dfrac{1}{\frac{l}{s} + 1}$:

$$\begin{aligned}
\frac{\beta C_D}{\left(t_{max}/c_{max}\right)^2} = -\frac{1}{\pi}\Bigg\{ & \frac{\beta \cot \Lambda}{\sqrt{1 - \beta^2 \cot^2 \Lambda}}\Bigg[- 2 \cosh^{-1} \frac{1 + \beta^2 \cot^2 \Lambda}{2\beta \cot \Lambda} - \left(\frac{l}{2s} + 1\right)^2 \cosh^{-1} \frac{1 + \left(\frac{l}{s} + 1\right)\beta^2 \cot^2 \Lambda}{\left(\frac{l}{s} + 2\right)\beta \cot \Lambda} + \\
& \frac{l}{4s} \frac{4(1 - \beta^2 \cot^2 \Lambda) + \frac{l}{s}(1 + \beta^2 \cot^2 \Lambda)}{1 - \beta^2 \cot^2 \Lambda} \cosh^{-1} \frac{1 + \left(\frac{l}{s} - 1\right)\beta^2 \cot^2 \Lambda}{\frac{l}{s}\beta \cot \Lambda} - \\
& \frac{l}{4s} \frac{4(1 - \beta^2 \cot^2 \Lambda) - \frac{l}{s}(1 + \beta^2 \cot^2 \Lambda)}{1 - \beta^2 \cot^2 \Lambda} \cosh^{-1} \frac{1 - \left(\frac{l}{s} + 1\right)\beta^2 \cot^2 \Lambda}{\frac{l}{s}\beta \cot \Lambda} - \\
& \left(\frac{l}{2s} - 1\right)^2 \cosh^{-1} \frac{1 - \left(\frac{l}{s} - 1\right)\beta^2 \cot^2 \Lambda}{\left(\frac{l}{s} - 2\right)\beta \cot \Lambda} + \\
& \frac{l}{2s} \frac{1}{\sqrt{1 - \beta^2 \cot^2 \Lambda}}\left(\sqrt{1 - \left(\frac{l}{s} + 1\right)^2\beta^2 \cot^2 \Lambda} - \sqrt{1 - \left(\frac{l}{s} - 1\right)^2\beta^2 \cot^2 \Lambda}\right)\Bigg] - \\
& 2 \sin^{-1} \beta \cot \Lambda + \cos^{-1}\left[\left(\frac{l}{s} + 1\right)\beta \cot \Lambda\right] - \cos^{-1}\left[\left(\frac{l}{s} - 1\right)\beta \cot \Lambda\right]\Bigg\}
\end{aligned} \tag{D5}$$

For $\dfrac{1}{\frac{l}{s} + 1} < \beta \cot \Lambda \leqq \dfrac{1}{\frac{l}{s} - 1}$:

$$\frac{\beta C_D}{(t_{max}/c_{max})^2} = -\frac{1}{\pi}\left\{\frac{\beta \cot \Lambda}{\sqrt{1 - \beta^2 \cot^2 \Lambda}}\left[\frac{l}{4s}\,\frac{4(1 - \beta^2 \cot^2 \Lambda) + \frac{l}{s}(1 + \beta^2 \cot^2 \Lambda)}{1 - \beta^2 \cot^2 \Lambda} \cosh^{-1} \frac{1 + \left(\frac{l}{s} - 1\right)\beta^2 \cot^2 \Lambda}{\frac{l}{s}\beta \cot \Lambda} - \right.\right.$$

$$\left(\frac{l}{2s} - 1\right)^2 \cosh^{-1} \frac{1 - \left(\frac{l}{s} - 1\right)\beta^2 \cot^2 \Lambda}{\left(\frac{l}{s} - 2\right)\beta \cot \Lambda} - 2 \cosh^{-1} \frac{1 + \beta^2 \cot^2 \Lambda}{2\beta \cot \Lambda} -$$

$$\left.\left.\frac{l}{2s}\,\frac{\sqrt{1 - \left(\frac{l}{s} - 1\right)^2 \beta^2 \cot^2 \Lambda}}{\sqrt{1 - \beta^2 \cot^2 \Lambda}}\right] - 2 \sin^{-1} \beta \cot \Lambda - \cos^{-1}\left[\left(\frac{l}{s} - 1\right)\beta \cot \Lambda\right]\right\} \tag{D6}$$

For $\dfrac{1}{\frac{l}{s} - 1} < \beta \cot \Lambda < 1$:

$$\frac{\beta C_D}{(t_{max}/c_{max})^2} = \frac{2}{\pi}\left\{\frac{\beta \cot \Lambda}{\sqrt{1 - \beta^2 \cot^2 \Lambda}} \cosh^{-1} \frac{\beta^2 \cot^2 \Lambda + 1}{2\beta \cot \Lambda} + \sin^{-1} \beta \cot \Lambda\right\} \tag{D7}$$

For $\beta \cot \Lambda \geqq 1$:

$$\frac{\beta C_D}{(t_{max}/c_{max})^2} = 1 \tag{D8}$$

APPENDIX E

EXPRESSIONS FOR INTERFERENCE PRESSURES ACTING ON BASE

The formulas in this appendix give the interference pressures (in coefficient form) acting along the base line in the plane of symmetry, that is, $x = c_{max}$ and $z = 0$.

Canted Arrangement

For the case where all the edges are subsonic, that is, $\beta \cot \Lambda < 1$, the formula is

$$\frac{\beta}{(t_{max}/c_{max})}\left(\frac{\Delta p}{q}\right)_{base\ int} = -\frac{2}{\pi(\beta \cot \Lambda - \beta \tan \theta)}\left[\frac{(\beta \cot \Lambda + \beta \tan \theta)^2}{\sqrt{4 - (\beta \cot \Lambda + \beta \tan \theta)^2}} \cosh^{-1} \frac{2 + (\beta \tan \theta + \beta \cot \Lambda)\left(\frac{y}{s}\right)\beta \cot \Lambda}{\beta \tan \theta + \left(1 + 2\frac{y}{s}\right)\beta \cot \Lambda} - \right.$$

$$\left. \frac{\beta^2 \cot^2 \Lambda}{\sqrt{1 - \beta^2 \cot^2 \Lambda}} \cosh^{-1} \frac{1 + \left(\frac{y}{s}\right)\beta^2 \cot^2 \Lambda}{\left(1 + \frac{y}{s}\right)\beta \cot \Lambda} - \frac{\beta^2 \tan^2 \theta}{\sqrt{1 - \beta^2 \tan^2 \theta}} \cosh^{-1} \frac{1 + \left(\frac{y}{s}\right)(\beta \cot \Lambda)\beta \tan \theta}{\beta \tan \theta + \left(\frac{y}{s}\right)\beta \cot \Lambda}\right] \tag{E1}$$

When the leading edge becomes sonic, that is, $\beta \cot \Lambda = 1$, equation (E1) reduces to

$$\frac{\beta}{(t_{max}/c_{max})}\left(\frac{\Delta p}{q}\right)_{base\ int} = -\frac{2}{\pi(1 - \beta \tan \theta)}\left[\frac{(1 + \beta \tan \theta)^2}{\sqrt{(1 - \beta \tan \theta)(3 + \beta \tan \theta)}} \cosh^{-1} \frac{2 + \frac{y}{s}(1 + \beta \tan \theta)}{1 + \beta \tan \theta + 2\frac{y}{s}} - \right.$$

$$\left. \frac{\beta^2 \tan^2 \theta}{\sqrt{1 - \beta^2 \tan^2 \theta}} \cosh^{-1} \frac{1 + \frac{y}{s}\beta \tan \theta}{\beta \tan \theta + \frac{y}{s}} - \sqrt{\frac{1 - \frac{y}{s}}{1 + \frac{y}{s}}}\right] \tag{E2}$$

For the condition where the leading edge is supersonic but the remaining edges are subsonic, that is, $\beta \cot \Lambda > 1$, $\beta\left(\frac{\tan \theta + \cot \Lambda}{2}\right) < 1$, the interference pressure is given by

$$\frac{\beta}{(t_{max}/c_{max})}\left(\frac{\Delta p}{q}\right)_{base\ int} = -\frac{2}{\pi(\beta \cot \Lambda - \beta \tan \theta)}\left[\frac{(\beta \cot \Lambda + \beta \tan \theta)^2}{\sqrt{4 - (\beta \cot \Lambda + \beta \tan \theta)^2}} \cosh^{-1} \frac{2 + \left(\frac{y}{s}\right)(\beta \cot \Lambda)(\beta \tan \theta + \beta \cot \Lambda)}{\beta \tan \theta + \left(1 + \frac{2y}{s}\right)\beta \cot \Lambda} - \right.$$

$$\left. \frac{\beta^2 \cot^2 \Lambda}{\sqrt{\beta^2 \cot^2 \Lambda - 1}} \cos^{-1} \frac{1 + \left(\frac{y}{s}\right)\beta^2 \cot^2 \Lambda}{\left(1 + \frac{y}{s}\right)\beta \cot \Lambda} - \frac{\beta^2 \tan^2 \theta}{\sqrt{1 - \beta^2 \tan^2 \theta}} \cosh^{-1} \frac{1 + \left(\frac{y}{s}\right)(\beta \cot \Lambda)\beta \tan \theta}{\beta \tan \theta + \left(\frac{y}{s}\right)\beta \cot \Lambda}\right. \tag{E3}$$

When the ridge line becomes sonic, that is, $\beta\left(\frac{\tan\theta + \cot\Lambda}{2}\right) = 1$ equation (E3) reduces to

$$\frac{\beta}{\left(t_{max}/c_{max}\right)}\left(\frac{\Delta p}{q}\right)_{base\ int} = -\frac{2}{\pi(\beta\cot\Lambda - \beta\tan\theta)}\left[2\sqrt{\frac{1-\left(\frac{y}{s}\right)\beta\cot\Lambda}{1+\left(\frac{y}{s}\right)\beta\cot\Lambda}} - \frac{\beta^2\cot^2\Lambda}{\sqrt{\beta^2\cot^2\Lambda - 1}}\cos^{-1}\frac{1+\left(\frac{y}{s}\right)\beta^2\cot^2\Lambda}{\left(1+\frac{y}{s}\right)\beta\cot\Lambda} - \right.$$

$$\left.\frac{\beta^2\tan^2\theta}{\sqrt{1-\beta^2\tan^2\theta}}\cosh^{-1}\frac{1+\left(\frac{y}{s}\right)(\beta\cot\Lambda)\beta\tan\theta}{\beta\tan\theta + \left(\frac{y}{s}\right)\beta\cot\Lambda}\right] \tag{E4}$$

For the condition in which both the leading edge and ridge lines are supersonic but the innermost edge is subsonic, that is, $\beta\left(\frac{\tan\theta + \cot\Lambda}{2}\right) > 1$ and $\beta\tan\theta < 1$, the pressure formula is

$$\frac{\beta}{\left(t_{max}/c_{max}\right)}\left(\frac{\Delta p}{q}\right)_{base\ int} = -\frac{2}{\pi(\beta\cot\Lambda - \beta\tan\theta)}\left[\frac{(\beta\cot\Lambda + \beta\tan\theta)^2}{\sqrt{(\beta\cot\Lambda + \beta\tan\theta)^2 - 4}}\cos^{-1}\frac{2+\left(\frac{y}{s}\right)(\beta\cot\Lambda)(\beta\tan\theta + \beta\cot\Lambda)}{\beta\tan\theta + \left(1+2\frac{y}{s}\right)\beta\cot\Lambda} - \right.$$

$$\left.\frac{\beta^2\cot^2\Lambda}{\sqrt{\beta^2\cot^2\Lambda - 1}}\cos^{-1}\frac{1+\left(\frac{y}{s}\right)\beta^2\cot^2\Lambda}{\left(1+\frac{y}{s}\right)\beta\cot\Lambda} - \frac{\beta^2\tan^2\theta}{\sqrt{1-\beta^2\tan^2\theta}}\cosh^{-1}\frac{1+\left(\frac{y}{s}\right)(\beta\cot\Lambda)\beta\tan\theta}{\beta\tan\theta + \left(\frac{y}{s}\right)\beta\cot\Lambda}\right] \tag{E5}$$

At the higher Mach numbers (where the inner edge becomes sonic or supersonic) the interference field does not affect the base region of the opposite panel.

Parallel Arrangement

For the parallel arrangement of bodies the expression for the interference pressure is

$$\frac{\beta}{\left(t_{max}/c_{max}\right)}\left(\frac{\Delta p}{q}\right)_{base\ int} = \frac{\beta\cot\Lambda}{\pi\sqrt{1-\beta^2\cot^2\Lambda}}\left[\cosh^{-1}\frac{1-\left(\frac{y}{s}+\frac{l}{s}\right)\beta^2\cot^2\Lambda}{\left(\frac{y}{s}+\frac{l}{s}-1\right)\beta\cot\Lambda} + \cosh^{-1}\frac{1+\left(\frac{y}{s}+\frac{l}{s}\right)\beta^2\cot^2\Lambda}{\left(\frac{y}{s}+\frac{l}{s}+1\right)\beta\cot\Lambda}\right] \tag{E6}$$

REFERENCES

1. Friedman, Morris D., and Cohen, Doris: Arrangement of Fusiform Bodies To Reduce the Wave Drag at Supersonic Speeds. NACA Rep. 1236, 1955. (Supersedes NACA RM A51I20 by Friedman and TN 3345 by Friedman and Cohen.)

2. Evvard, John C.: Distribution of Wave Drag and Lift in the Vicinity of Wing Tips at Supersonic Speeds. NACA TN 1382, 1947.

3. Puckett, Allen E.: Supersonic Wave Drag of Thin Airfoils. Jour. Aero. Sci., vol. 13, no. 9, Sept. 1946, pp. 475-484.

TABLE I.- SUMMARY OF CASES TREATED, MATHEMATICAL CONDITIONS, AND APPLICABLE POTENTIAL EXPRESSIONS

Case	Description	Mathematical conditions	Applicable potential expressions
I	All edges subsonic	$\beta \cot \Lambda < 1$	ϕ_{1B}, ϕ_{2B}
II	Leading edge supersonic but other edges subsonic	$\beta \tan \theta + \beta \cot \Lambda < 2$ $\beta \cot \Lambda > 1$	ϕ_{1A}, ϕ_{2A}, ϕ_3
III	Only inner edge subsonic	$\beta \tan \theta < 1$ $\beta \tan \theta + \beta \cot \Lambda > 2$	ϕ_{1C}, ϕ_3, ϕ_4
IV	All edges supersonic	$\beta \tan \theta > 1$	ϕ_3, ϕ_4

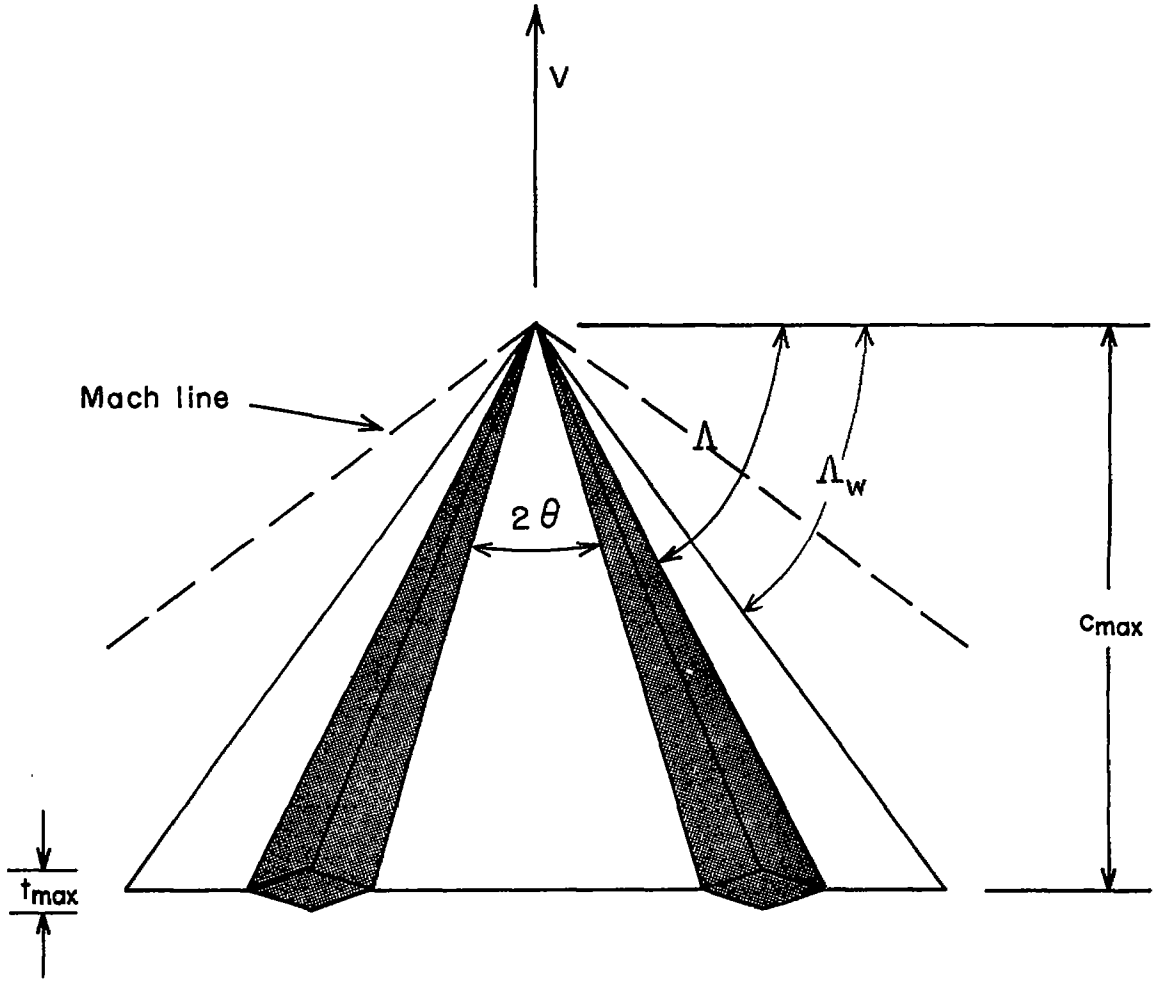

Figure 1.- Sketch indicating canted arrangement embedded in a delta wing and pertinent parameters used in analysis.

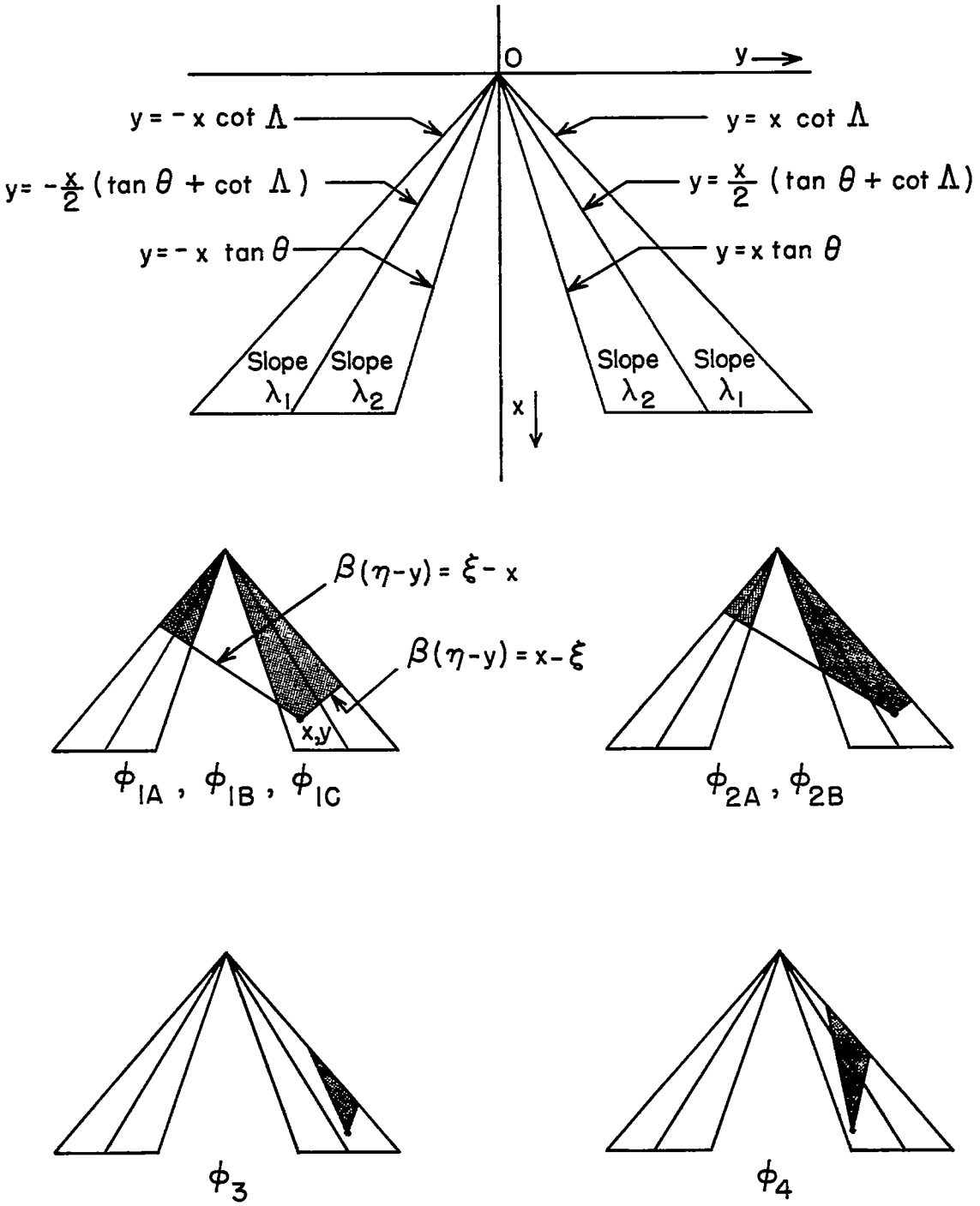

Figure 2.- Areas of integration and mathematical data required to obtain the various velocity potentials.

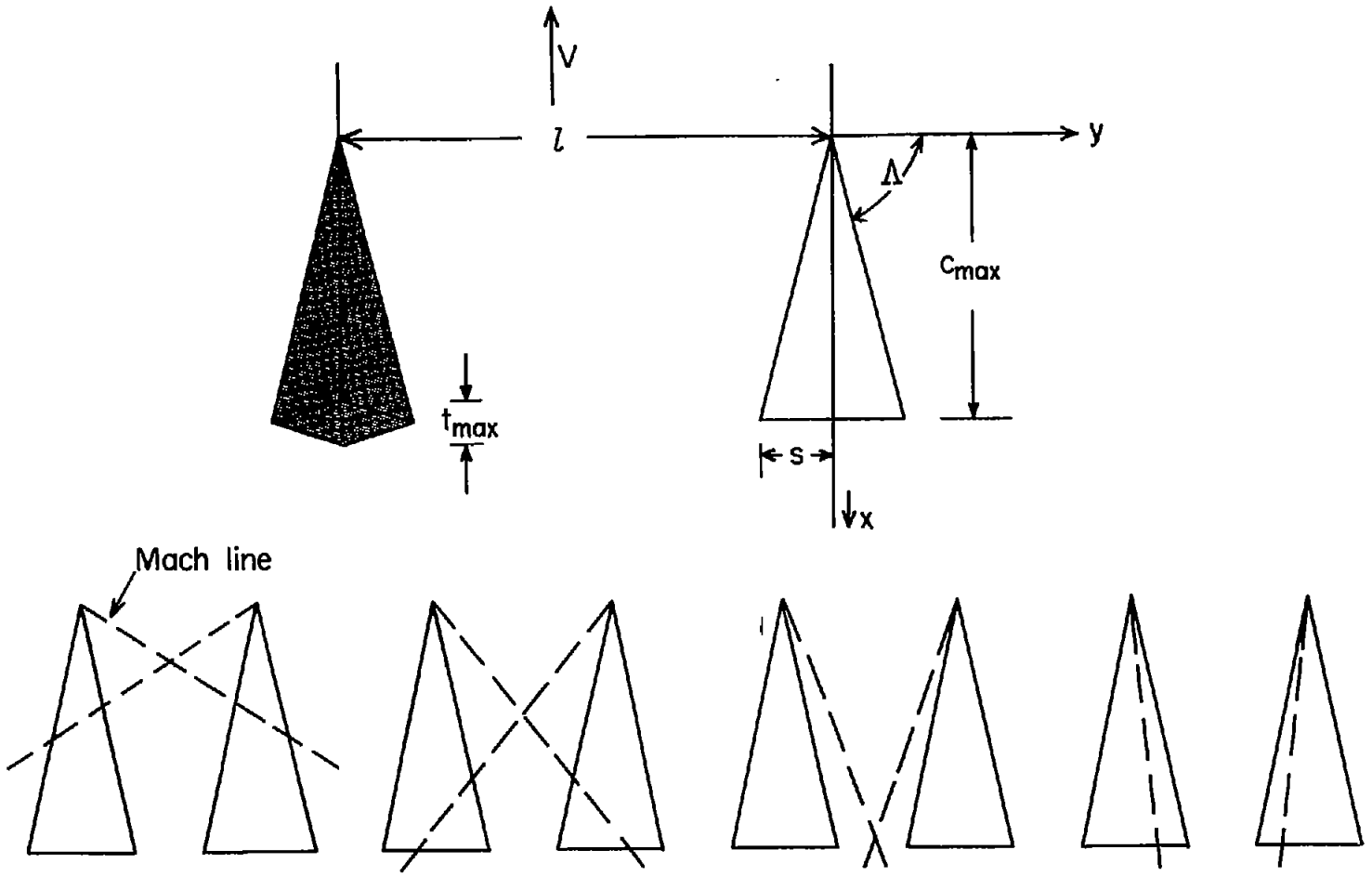

Figure 3.- Pertinent geometry for parallel arrangement of surfaces and sketches indicating various combinations possible for arbitrary values of Mach number, aspect ratio, and distance parameter l/s.

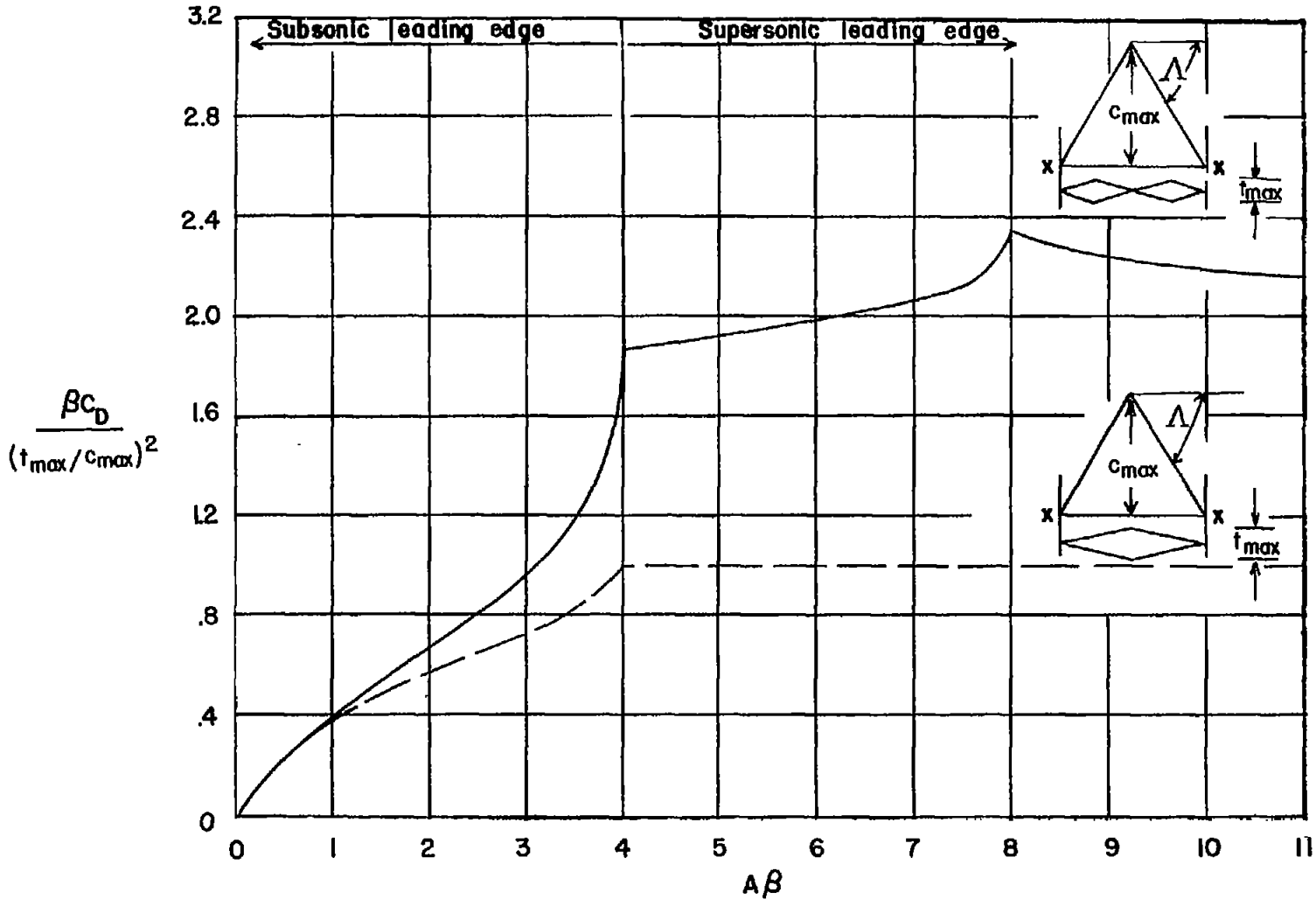

Figure 4.- Variation of wave-drag coefficient with aspect-ratio—Mach number parameter for two surfaces of delta plan form.

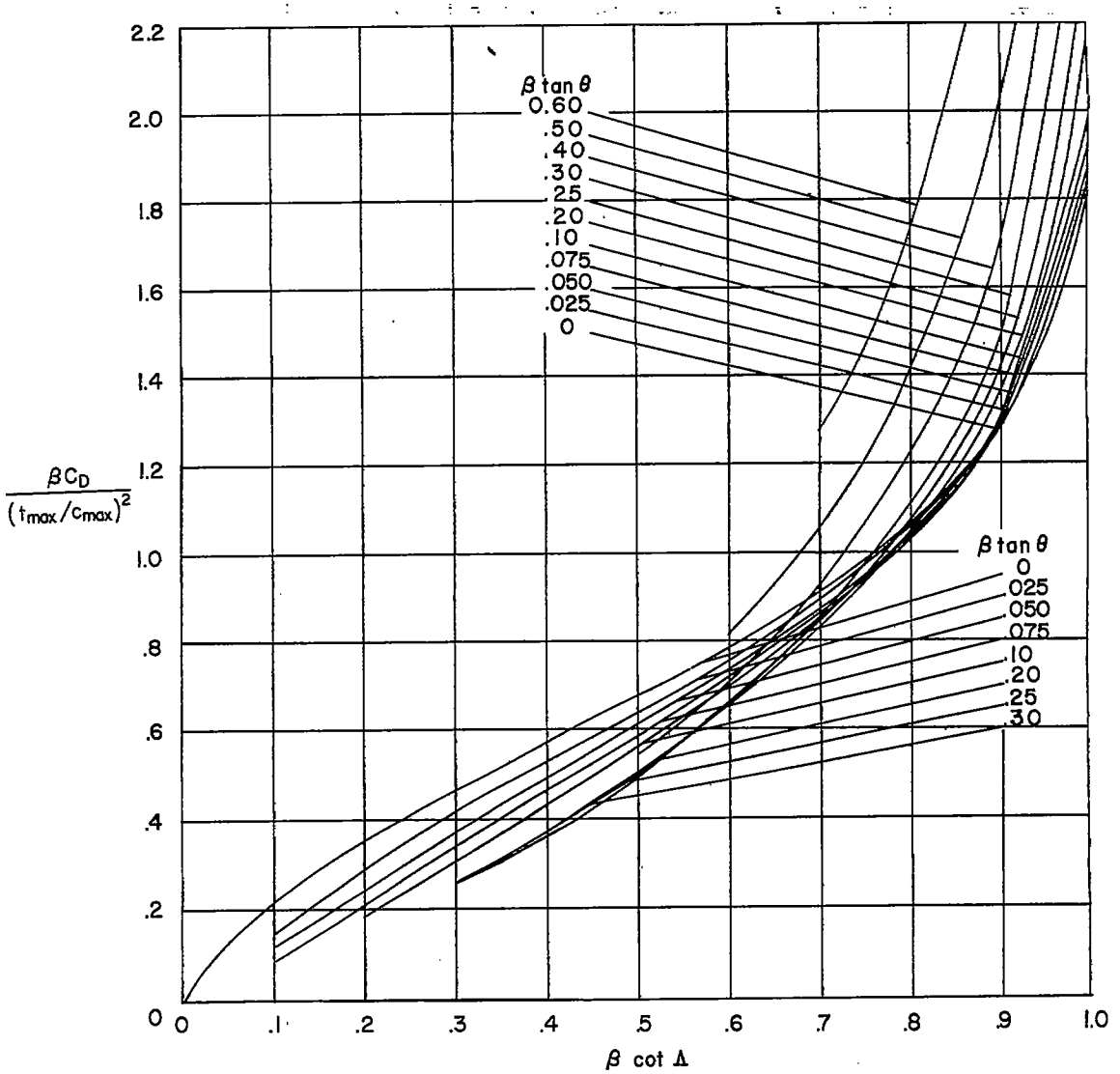

Figure 5.- Variation of wave-drag coefficient with Mach number-sweepback parameter for canted arrangement of surfaces.

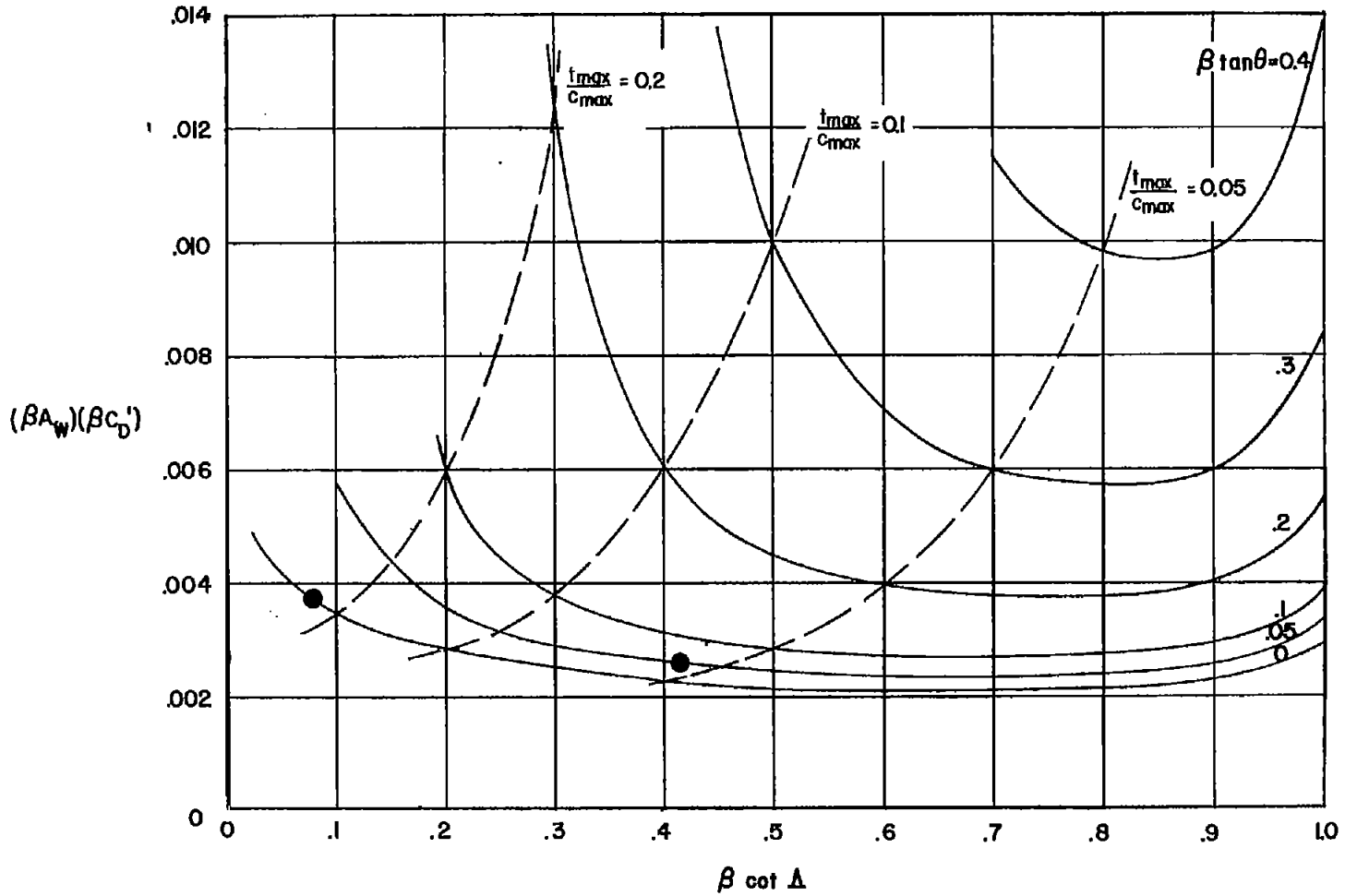

Figure 6.- Variation of wave-drag coefficient with Mach number-sweepback parameter for a given volume condition $\frac{3\beta V_B}{(c_{max})^3} = 0.02$ and several thickness ratios. (C_D' based on area of a delta wing with aspect ratio A_w.)

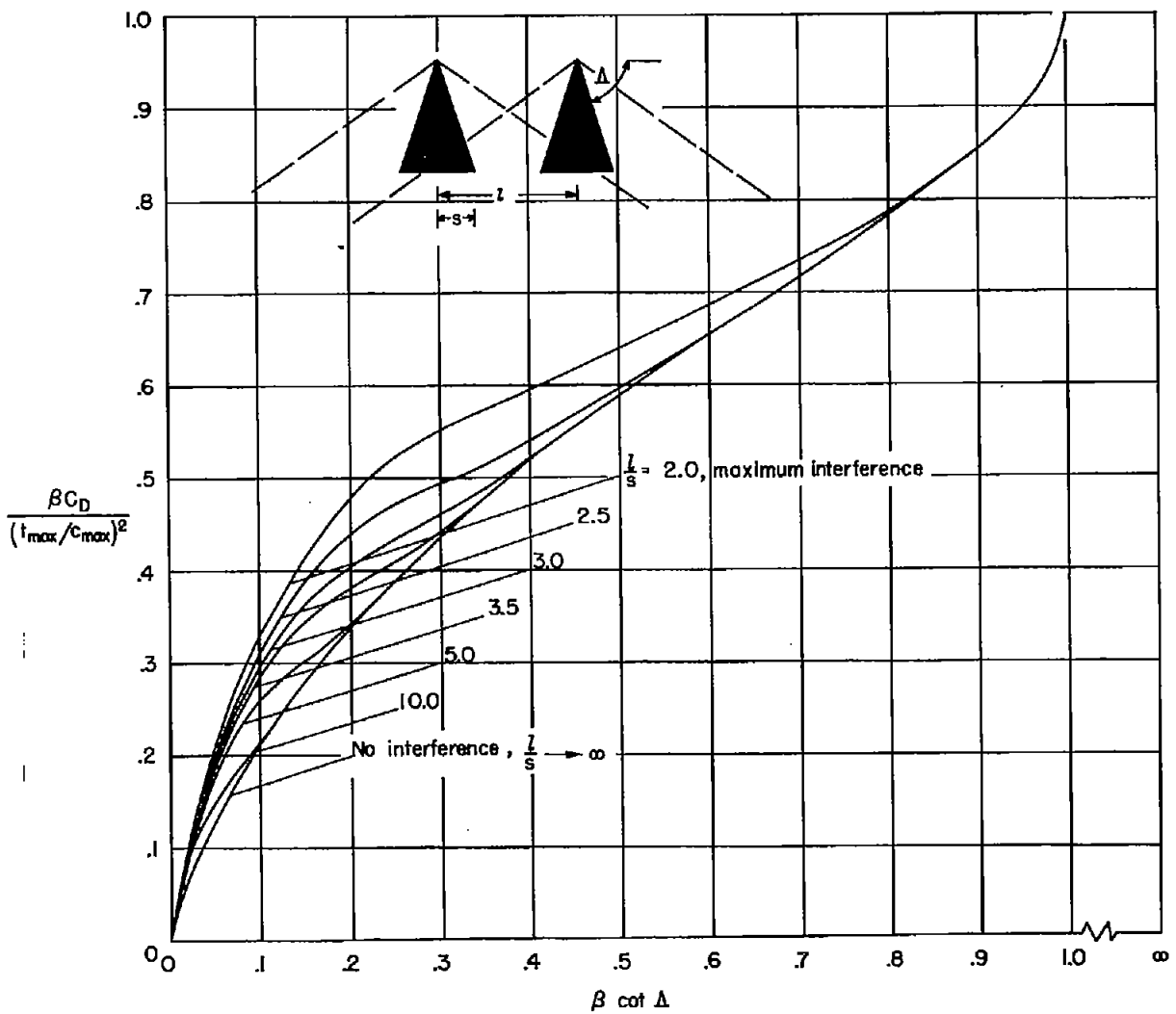

Figure 7.- Variation of wave-drag coefficient with several parameters for the parallel arrangement of surfaces.

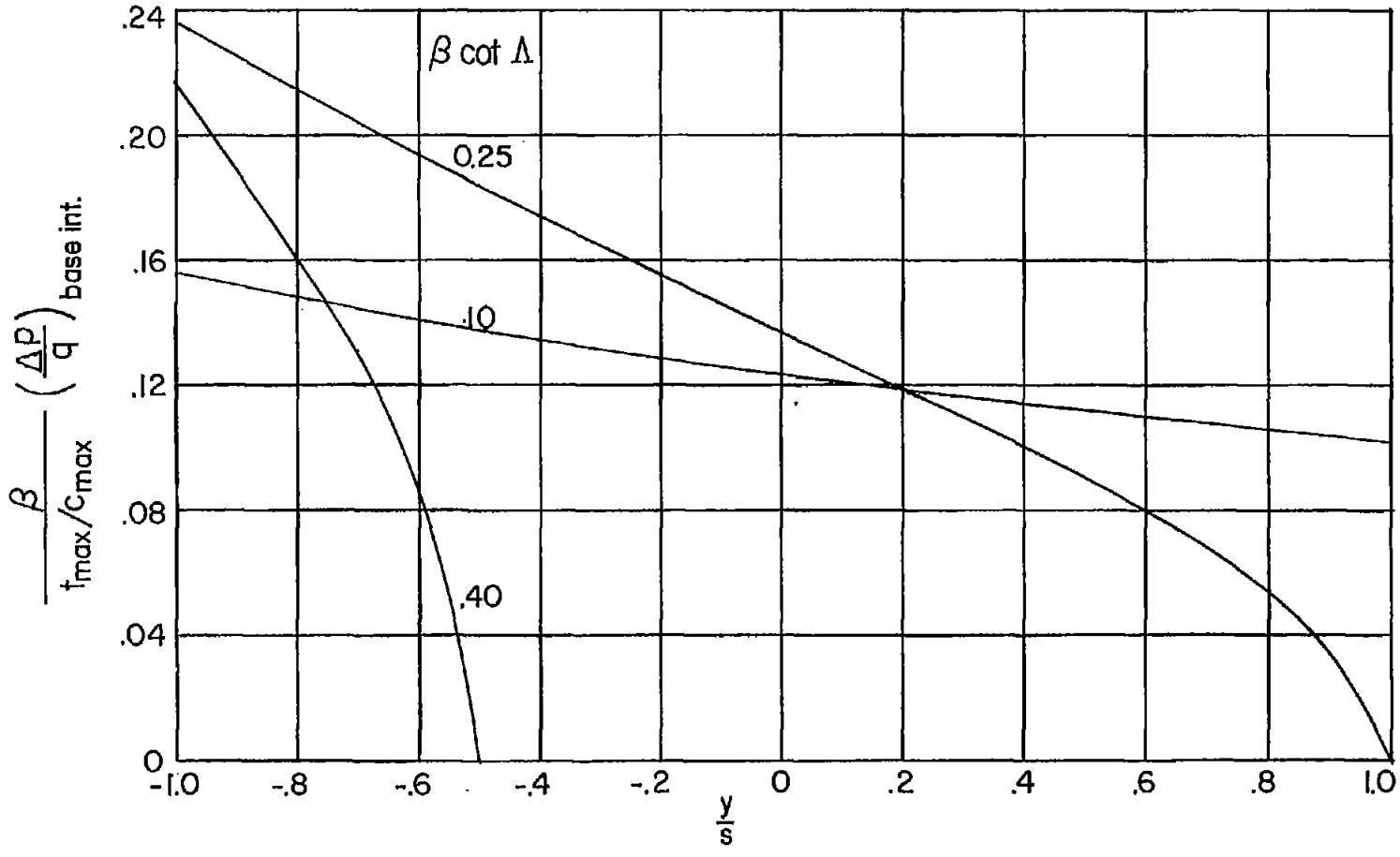

Figure 8.- Illustrative variations of the interference pressures acting along the base of one panel due to the presence of the opposite panel for the parallel arrangement of bodies. $l/s = 3.0$; $z = 0$; $x = c_{max}$.

NACA - Langley Field, Va.